Carbohydrate Polymers 232 (2020) 115813

Contents lists available at ScienceDirect

Carbohydrate Polymers

journal homepage: www.elsevier.com/locate/carbpol

Designation of chitosan nano-vaccine based on *MxiH* antigen of *Shigella flexneri* with increased immunization capacity

Farhad Gilavand[a], Abdolrazagh Marzban[b], Gholamhossein Ebrahimipour[a], Neda Soleimani[a], Mehdi Goudarzi[c,*]

[a] Department of Microbiology and Microbial Biotechnology, Faculty of Life Sciences and Biotechnology, Shahid Beheshti University, Tehran, Iran
[b] Razi Herbal Medicines Research Center, Lorestan University of Medical Sciences, Khorramabad, Iran
[c] Department of Microbiology, School of Medicine, Shahid Beheshti University of Medical Sciences, Tehran, Iran

ARTICLE INFO

Keywords:
Shigella flexnerii
Mxi hantigen
Chitosan nanoparticles
Infection challenge assay

ABSTRACT

Shigella flexneri is a gram-negative pathogen that causes shigellosis in humans and primates. *MxiH* antigen is known as one of the invasive factors in most Gram-negative bacteria consisting of a needle-like structure in the main backbone of the type 3 secretory system. Recombinant *MxiH* antigen was produced by *E. coli* BL21 and purified antigen was loaded into chitosan nanoparticles (CS-*MxiH*). After 20thand 55th of intranasal vaccinations, the titers of IgG, IgA, IL-4, and IFN-γ were evaluated. The results indicated the successful synthesis of CS nanoparticles followed by the effective loading of *MxiH* antigen. The results of animal experiments showed that the intranasal administration of CS-*MxiH* increased IgG and IgA compared to control groups. Increased levels of IL-4 and IFN-γ in groups immunized with CS-*MxiH* are probably due to the activation of plasmacytoid and myeloid cells presenting antigen in nasal epithelial mucosa and stimulating B cells.

1. Introduction

Shigellosis is an acute type of bloody diarrhea in humans, caused by *Shigella* genus (Kotloff et al., 2018). *Shigella* refers to the facultative gram-negative bacilli, which include various species, including *S. dysentery*, *S. flexneri*, and *S. sonnei*. In fact, the main hosts of *Shigella* genus are only humans and primates. This bacterium transmitted to humans with high virulence so that, only 10 organisms can be fatal for children under 5-year of age (Levine et al., 2007). However, Shigellosis is a self-limiting infection, which usually heals without antibiotic therapy within 7 days. However, in certain cases, individuals with immunedeficiencies and children with *shigella* infection can be at risk (Barry et al., 2013; Kotloff et al., 2018).

The target tissue of the *Shigella* invasion is the basal layer of the epithelium and the lumen of the colon. Although the specific receptors on B cells for binding *shigella* are not known yet, bacterial effector proteins are capable to bind α5β1 integrins (Camacho et al., 2013). After the bacteria pass through the M cells, they are phagocytosed by antigen-presenting cells (APCs) such as macrophage and dendritic cells that located in the propria tissue. After that, the bacterium escapes from the phagosome by an invasive protein-dependent process and enters the cytoplasm of the APCs cell. Then, they induce apoptosis in the macrophage by activating caspase 1 and cause the release of inflammatory mediators. Subsequently, invading bacteria are colonized on the lateral surface of epithelial cells, induced colon epithelial cells to produce complex inflammatory responses. Therefore, destruction of epithelial cells following shigella infection and subsequent immune responses to colon ulcers, mucus damage, and bloody stools are the main characteristic of shigellosis (Kaminski & Oaks, 2009; Kotloff et al., 2018).

The type 3 secretory system (TTSS3 or injectisome) is a common pathogenic mechanism in gram-negative bacteria that encoded by the plasmid. The TTSS3 consist of a needle-like structure or syringe with repeated *MxiH* antigenic units that covered by Ipa antigens D, B, and C located at the needle tip. The number of TTSS3 is estimated 50–100 per bacterial cell. Invasion of colon epithelial cells through the TTSS3 is found in all *Shigella* pathogenic serotypes which injected effector molecules into the host cells (Bohn et al., 2019; Martinez-Becerra et al., 2012).

MxiH is a 25-nm needle-like subunit protruding from the bacterial cell surface. *MxiH* protein consists of 83 amino acids with a molecular weight of 9.26 kDa that processes antigenic properties and stimulates antibody production (Kaminski & Oaks, 2009).

Despite extensive research to immunize people against *Shigella*

* Corresponding author.
E-mail addresses: Farhadgilavand@yahoo.com (F. Gilavand), Marzban86@gmail.com (A. Marzban), G-Ebrahimi@sbu.ac.ir (G. Ebrahimipour), N_soleimani@sbu.ac.ir (N. Soleimani), gudarzim@yahoo.com (M. Goudarzi).

https://doi.org/10.1016/j.carbpol.2019.115813
Received 14 November 2019; Received in revised form 18 December 2019; Accepted 29 December 2019
Available online 31 December 2019
0144-8617/

infection, an effective and safe vaccine for the prevention of *Shigellosis* is still not available (Ashkenazi & Cohen, 2013). To date, vaccines made against shigellosis have three forms: attenuated living, dead bacteria, and antigenic (subunit) vaccines. Components of the bacterial structure that have been used to design subunit vaccines included bacterial toxins, IpaD, IpaC, IpaB, LPS antigens or their combination. The importance of this study is the use of *mxiH* antigen (subunits forming the injectisome system) to design effective vaccines incorporated into CS nanoparticles (Ashkenazi & Cohen, 2013; Kaminski & Oaks, 2009).

Several studies have been conducted to establish a safe and effective *Shigella* vaccine. Vaccination via mucosal tissue, particularly intranasal, appears to enhance the effectiveness of the immune response to Shigella infection. A unique feature for immune responses at the mucosal surfaces is the production of sIgA and their transmission to the intestinal epithelium(Kaminski & Oaks, 2009; Levine et al., 2007).

Mucosal vaccines induce systemic and mucosal immunity, leading to an increased immune response at low doses. Despite the unique advantages of intranasal immunization, this reveals to be insufficient for stimulating the immune system since most antigenic macromolecules are unable to pass the nasal mucosal barrier (Taranejoo et al., 2011). Other factors, such as degradation of antigens by enzymes and entrapment of antigens in mucosal secretions, may limit the access of nasal-associated lymphoid tissue (NALT) to the antigen (Kang et al., 2007). Various strategies have been used to increase mucosal immune responses to make antigen administration more effective through the nose. The use of nanocarriers is one of the effective ways to prolong the duration of antigen residence in the nasal cavity for delivery to M-cells and antigen-presenting cells (APCs) (Amidi et al., 2006).

CS is a suitable biopolymer for the delivery of drugs and antigens (Ashrafi et al., 2019).CS-based nanoparticles have mucosal adhesive properties and thereby increase bioavailability and antigen uptake. CS nanoparticles have been used in numerous studies as a system of delivery of specific antigens to intestinal M-cells, dendritic cells, as well as increased loading capacity in mucosal immunization (Fasihi-Ramandi et al. 2018).

Akbari et al. (2019) loaded *Shigella flexneri*'s recombinant IpaD antigen into N-trimethyl CS (TMC) nanoparticles and orally vaccinated Guinea pigs. Their results showed an increase in serum levels of IgG and sIgA. Jahantigh et al. (2014) greatly improved humoral immune stimulation and immunoglobulin Secretion by loading IpaD antigen of *Shigella flexneri*onto the CS nanopolymer. In the same research, the IpaD antigen loaded with CS nanofibers did not have a significant effect on humoral immune levels, especially IgA.

In this study, recombinant *MxiH* protein was produced in *E. coli* and purified using NTA (His-tag) system. Then, *MxiH* was loaded in CS nanoparticles and CS-*MxiH* nanoparticles were studied for their stability, loading capacity, size, and surface charge. Finally, immunization potential of the nanoparticles was examined in vivo in mice followed by evaluating the level of IFN-γ, IL-4, IgA, and IgG.

2. Materials and methods

Chemical materials and media cultures were purchased from Merck company. ELISA kits for cytokine assay were procured from Sinaclon DNA extraction, PCR and plasmid extraction were prepared from Sinaclon and Kiagen and molecular markers purchased from Fermentas.Low molecular weight CS with deacetylation grade of 85 % was purchased from Sigma, Germany.

2.1. Strains, plasmids, and culture conditions

The host bacterial strain used in this study was *E. coli* BL21 that was procured from Pasteur Institute, Tehran, Iran. *S. flexneri*, Serotype 1a (PTCC 1234) was provided from IROST, Tehran, Iran. The *MxiH* gene was extracted from the bacterial genome and amplified by PCR method. Finally, the *MxiH* gene was ligated in a plasmid, PET28a, (Novagen, Madison, USA).

2.1.1. Screening of recombinant clones and Confirmation of MxiH gene

After transformation of pET28a-*MxiH* vector in *E. coli* BL21 as the host, screening the positive colonies were screened by colony PCR method. In this step, from the overnight bacterial culture on the LB broth supplemented with 40 μg/ml kanamycin, 15 colonies were taken to extract the transformed plasmid pET28a containing *MxiH* gene. The plasmid was extracted from the colony samples using a plasmidextraction and purification kit. The presence of the *MxiH* gene was investigated by two specific primers (forward: 5′-ATTCATATGTCTGTTA CCGTTCCG-3′ and reverse: 5′-GTGGATCCGACGGAAGTTCTGGA-3′) followed by gel electrophoresis on 1 % agarose. *MxiH* gene was amplified according to the following program: initial denaturation at 95 °C for 5 min, 30 cycles of denaturation at 95 °C for 35 S, extension at 72 °C for 30 s and final extension at 72 °C for 10 min.

2.1.2. Expression of MxiH gene

The recombinant strain *E. coli* BL21 (DE3) containing pET28a-*MxiH* plasmid was selected for expression of *MxiH* protein. The host bacterium was grown in the LB broth supplemented with 40 μg/ml kanamycin (sigma) by incubating at 37 °C with shaking 150 rpm. When the bacterial cell density (OD 600 nm) reached to 0.5-0.6, induction of gene expression was conducted by adding 1 mM Isopropyl β-D-1-thiogalactopyranoside (IPTG) to the culture broth medium. To complete protein expression, culture medium was incubated at same conditions for 24 h.

After that, the broth culture was centrifuged at 6000 rpm for 15 min. The bacterial cells were broken by lysis buffer (Urea 8 M) combined with a soft sonication. Then, the cell lysate containing protein was taken and analyzed using SDS-PAGE on 12 % polyacrylamide gel with a 6 % stacking gel by comparing it with a protein weight marker (Fermentas, 200 kDa). To visualize the protein bonds, the PAGE was stained by coomassie blue R-250 for 1 h and then the gel was treated by a destaining solution (15 % methanol and 10 % acetic acid) for 6 h (Khanifar et al., 2019; Marandi et al., 2019).

2.1.3. Purification of recombinant protein MxiH

The 6His-*MxiH* recombinant protein was purified by affinity chromatography using Ni-NTA resin (Qiagen, USA) according to the manufacturer protocol.

A volume of 100 ml of overnight-grown bacteria was centrifuged at 6000 rpm at 4 °C for 15 min. The pellet was disrupted by a 5 ml lysis buffer solution and slowly shaken at room temperature for 45 min for completing the cell lysis. After that, the lysate was centrifuged at 14,000 rpm at 4 °C for 15 min. The supernatant containing recombinant protein was subjected to a Ni-NTA column and the flow-through was collected. Washing buffer 1 (30 mm imidazole) was added to the column to remove remaining unbound proteins and finally, the column was eluted with 2 ml of elution buffer (300 mM imidazole along with glycerol 5 %) for 3 times for completing the elution process.

The dialysis buffer PBS (Merck Co., UK) was used in order to remove the imidazole from the protein solution. In each step the flow-through was collected. The collected samples were analyzed by SDS-PAGE (12 %) as aforementioned protocol (Kazemi et al., 2016; Khanifar et al., 2019). Bradford assay was conducted to determine protein concentration in the samples (Bradford, 1976).

2.2. Western blotting analysis

The separated protein by SDS-PAGE was transferred to a nitrocellulose membrane by Bio-Rad Mini Protean II apparatus. To transfer the protein bond, a transfer buffer consisted of 39 mM glycine, 48 mM Tris-base, 0.037 % SDS, and 20 % methanol was used. The membrane was treated to the blocking buffer (5 % skim milk dissolved in phosphate-buffered saline, pH7.3) at 4 °C for 12 h. after that, the

membrane was incubated in anti-His-tag antimouse-IgG in 1:1000 dilution factor antibody in the TPBS (0.05 % tween-20 dissolved in PBS) followed by gentle shaking at 37 °C for 1 h. The membrane was then washed with TPBS for three times and then incubated in1:50,000 dilution of HRP-conjugated goat anti-mouse IgG antibody, with gentle shaking at 37 °C for 1 h. The blotted proteins were detected using chromogenic reaction with 3,3′-diaminobenzidine, 0.06 % (DAB) (Sigma) (Khanifar et al., 2019).

2.2.1. Preparation and characterization of CS-MxiH

CS nanoparticles were synthesized by the ionic gelation of CS with sodium tripolyphosphate (TPP) (Fasihi-Ramandi et al., 2018; Khanifar et al., 2019). CS in acidic solution is positively charged due to the presence of amine groups in its structure. CS nanoparticle was prepared by dissolving 0.4 % CS in acetic acid solution (1 %). For loading the *MxiH* protein, 0.1 mg/ml of *MxiH* was added to CS-acetic acid solution. Gelation was promoted by dropwise addition of the TPP stock solution (0.5 %) on magnetic stirrer at 1000 rpm for 1 h at room temperature. The nanoparticles were separated by centrifugation at 14,000 rpm and 4 °C for 20 min and freeze-dried. The freeze-dried nanoparticles was weighed and kept at 4 °C until further studies. To elucidate the change of CS nanoparticles after the loading, its size and morphology were analyzed using SEM, DLS and Zeta potential.

2.3. Loading capacityandrelease assay

The release of *MxiH* antigen from CS nanostructure was studied for 72 h after suspending CS-*MxiH* in 6 ml of 0.1 M PBS (pH 7.4) with stirring at 100 rpm at 37 °C. At 6 h intervals, 0.5 ml of the suspension was taken and centrifuged at 14000 rpm for 30 min and the protein released into the supernatants measured by Bradford protein assay (Bradford, 1976). To remain volume of sample, the same volume of PBS buffer was added to it. A blank was provided as non-loaded CS-NPs (Amini et al., 2017).

Loading capacity (LC) of CS for *MxiH* antigen was determined by an indirect method by measuring the amount of antigen that remained in supernatant. A certain amount of nanoparticles was centrifuged at 14,000 rpm for 30 min and the antigen in the supernatant was measured by Bradford protein assay. An unloaded CS nanoparticles suspension was applied as the control to remove the interference of CS. Loading capacity (LC) values were calculated as follows (Najminejad et al., 2019):

$$\text{Loading efficiency (\%)} = \frac{[(\text{Total antigen}) - (\text{antigen in the supernatant})]}{(\text{Total antigen})} \times 100$$

2.4. Animal immunization assay

Animal experiments were approved by the institutional animal care and use committee of ShahidBeheshti University of Medical Sciences (animal ethic permission code: IR.SBMU.MSP.REC.1396.376). The experimental procedures complied with the guide for the care and use of laboratory animals. Therefore,all experiments were carried out with minimum suffering to animals. Total 60 male BALB/C mice (21 day-aged) were purchased from Pasteur Institute of Iran. Animals were divided into 2 similar set experimental groups that 30 animals were selected for immunization response assay and the remaining 30 animals were considered for challenging assay after 3 times immunization by all antigenic formulations. Both set were divided into 5 groups of 6 animals with the following conditions in the parallel experiment:

Group 1 and 2 received only CS nanoparticles and phosphate buffer solution (negative control), respectively; group 3 was given Cs-*MxiH* nanoparticles (CS-*MxiH*); group 4 was challenged with *MxiH* antigen; group 5 received complete Freund's adjuvant-*MxiH* (Adj-*MxiH*) (positive control). To each mouse, 0.2 ml of related formulation was injected intranasally three times, on the first, 20th and 55th days. Blood sampling obtained from mice after 72 h of the second and third injections. The sera were separated from the blood samples by centrifugation at 2000 rpm for 5 min and stored at −20 °C until use.

2.5. Determining the IgG and IgA titer by ELISA

To assess the humoral immune response to *MxiH* antigen, an enzyme linked immunosorbent assay (ELISA) method (Zymed Laboratories Inc., San Francisco, USA) was applied. Briefly, 96-well microplates (Nunc) were coated with 100 µl of 5 µg/ml of *MxiH* and incubated overnight at 4 °C. The wells without antigen and without antibody were used as controls. Microplates were washed in PBS buffer containing 0.05 % tween-20 (PBS/T) and blocked with gelatin (5 % w/v) in PBS/T. samples of all groups (immunized and controls) were serially diluted to 1:500 in PBS/T. The diluted samples were added to the microplates and incubated at 37 °C for 1 h with gentle shaking. After that, secondary antibody (1:2500) was added to the wells and incubated at 37 °C for 1 h. After removing the unbound serum antibodies by washing (3 times in PBS/T) from the microplates, HRP goat anti-mouse IgG (1:50,000) or HRP goat anti-mouse IgA antibodies (1:10,000) was added to the microplates. Then they incubated at 37 °C for 30 min and washed 3 times in PBS/T for removing unbound antibodies. To make the reaction, the substrate of the enzyme HRP, O-phenylenediaminedihydrochloride (OPD) was added to each well. Then, the microplates were incubated into a dark place at room temperature for 15 min. Finally, the reaction was stopped by the addition of H_2SO_4 and the absorbance of the samples read by ELISA reader at 492 nm.

2.6. Measurement of IL-4 and IFN-γ cytokines

To determine cytokine immune response, the levels of IL-4 and IFN-γ was assessed 2 weeks after the final immunization. For this purpose, 4 mice of each group were sacrificed and their spleens were aseptically collected. To isolate the splenocytes, the spleens were homogenized in 1 ml of phosphate buffer saline (PBS), then the suspended phase was removed and transferred to another tube containing 4 ml ficoll (HistoPaque-1083). The tube was mixed carefully and slowly, then the top layer was collected into a new 15 ml tube. After that, cell pellet was resuspended in the fresh RPMI 1640 and counted the splenic mononuclear cells, they were seeded (3×10^5 cell/well) in a 96-well plate. Antigen stimulation was separately carried out with adding 10 µl of each stimulant solution including *MxiH* (5 µg/ml), CS-*MxiH* (10 µg/ml), CS (10 µg/ml), Adj-*MxiH* (10 µg/ml) and PBS buffer (negative control). The microplates were incubated at 37 °C for 72 h in 5 % CO_2 incubator. The level of IFN-γ and IL-4 was determined using quantitative ELISA assay kits (BD Biosciences, San Jose, CA). The assessment was performed as described by the manufacturer's protocol.

2.7. Challenge assay of the immunized mice

Challenge assay was carried out on three groups of 10 members that immunized by *MxiH*, CS-*MxiH*, and Adj-*MxiH*. Negative control was a 10-member group without immunization. The animals were subjected to challenge with the infection of *S. flexneri*, Serotype 1a (PTCC1234). The animals were intranasally infected by 4×10^6 Cfu/mouse. The survival rate of all groups was determined for 10 days. For this purpose, the bacterium was grown on 5 ml of trypticase soy broth (TSA) (Difco) broth and incubated for 12 h at 37 °C. Then, the bacterial culture was centrifuged at 4000 rpm for 10 min. The cell pellet was dissolved in 1 m of PBS and a lethal dose of bacterial suspension (4×10^6 bacterial cell/mouse) was intranasally injected to the mice. To scrutinize the immunity level against a lethal infection of *S. flexneri*, the survival curves of all groups were constructed for 10 days post-challenge. The survival

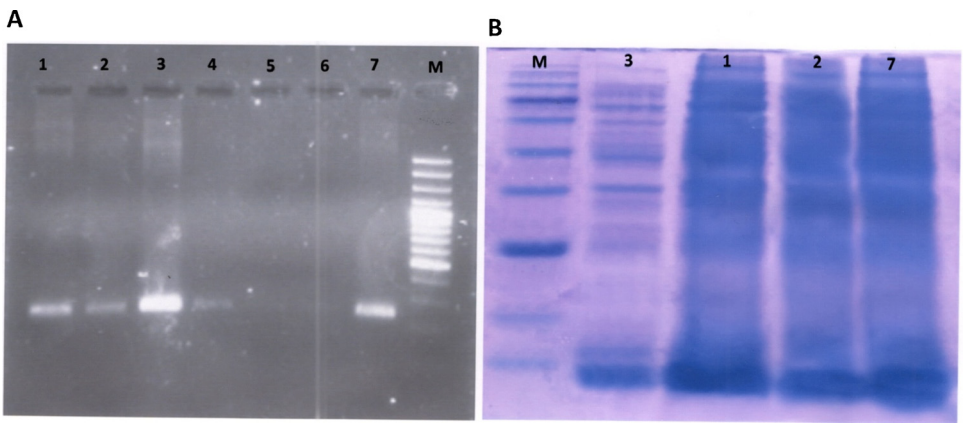

Fig. 1. Screening the recombinant colonies and expression of *MxiH* gene. A. PCR product obtained from seven different colonies on the agarose gel: Lanes 1–4 and 7 exhibit to be recombinant containing pET28a-*MxiH* (positive), while lane 5 and 6 show no PCR product within *MxiH* band area (negative); lane M shows molecular weight ladder. B:SDS-PAGE gel exhibits the profile of protein expression for positive colonies. Lanes 1–3 and 7 show the presence of *MxiH* protein band at 10 kDa compared to weight markers (M).

percentage (%) all groups was calculated in comparison with non-immunized control group.

2.8. Statistical analysis

The data were presented as the mean ± standarddeviation (SD) calculated from three independent experiments. Analyses were performed using GraphPad Prism 5. Multiple comparisons were also performed using Tukey test for on one-way ANOVA test. Significant level was considered at P-values < 0.05.

3. Results

3.1. Confirmation of transformation by PCR and SDS-PAGE

Seven independent colonies were subjected to amplification using PCR with specific primers for the *MxiH* gene (Fig. 1A). The transformed colonies were identified by electrophoresing PCR products on 1 % agarose gel. Expected gene fragments were visualized as a 252 bp band area compared to the DNA ladder marker. Among the recombinant colonies, 2 different colonies (lanes of 5, 6) showed no PCR band on the gel. The positive colonies were selected to study the *MxiH* gene expression.

After cultivation of the colonies in LB broth medium in aforementioned conditions, the expression of recombinant protein was elucidated by SDS-PAGE analysis. The result was shown that the *MxiH* recombinant protein was expressed at the 10 kDa weight area as compared to protein weight marker (Fig. 1B).

3.2. Purification of the recombinant MxiH protein using Ni-NTA column

Based on the colony PCR screening and primary evaluating the *MxiH* expression, positive colony number 3 was selected for further studies. As mentioned in previous section, *MxiH* expression was obtained by induction of 1 mM IPTG in an overnight incubation at 37 °C. The related protein was purified using Ni-NTA beads. As shown in Fig. 2, recombinant *MxiH* protein along with 6-His fused residue can be observed within 10 kDa band area on the SDS-PAGE (Fig. 2A). Western Blotting technique was conducted using anti-His antibody to elucidate the expression of *MxiH* recombinant protein. The presence of *MxiH* protein was confirmed by10 kDa on the western blotted paper (Fig. 2B).

3.3. Nanoparticles characterization

Nanoparticles were characterized based on the particle size analysis by size distribution prior to antigen loading and after that, *MxiH* was loaded to CS nanoparticles. According to the analysis as showed in Fig. 3A and B, particle size range decreased by condensing the *MxiH* antigen and also polydispersity index (PDI) decreased from 0.54 in CS to 0.32 in CS-*MxiH*.The SEM image showed that the CS-*MxiH* nanoparticles ranged from 50 to 300 nm (Fig. 4A, B), confirming the results obtained from DLS. Nonetheless, contrary to the DLS analysis, the size of the nanoparticles did not change substantially with the loading of *MxiH* in CS.

The external surface of the nanoparticles studied by SEM showed that they were spherical in size of approximately 100 nm. The CS-*MxiH* nanoparticles were characterized by having relatively smooth surfaces while the CS nanoparticles appeared relatively rough. (Fig. 4). Zeta potential showed the surface charge of CS nanoparticles in the positive range (Fig. 3C and D).

3.4. Encapsulation and release assay

The encapsulation efficiency was calculated to be 67 % for 0.1 mg/ml of *MxiH* antigen loaded into 0.3 mg/ml of CS nanoparticles. The in vitro release assay of *MxiH* antigen showed that about 57 % of the antigen was released during 72 h (Fig. 5).

3.5. Titration of serum IgG and IgA

Fig. 6 shows ELISA results of IgG and IgA titration from 3 groups including immunized mice including MxiH, CS-*MxiH* and Adj-*MxiH* compared to control groups (CS and PBS). The results showed no significant difference in IgG titer for CS-*MxiH* and Adj-*MxiH* groups. The titer of IgG in *MxiH*-immunized group was significantly lower than the CS-*MxiH* group and higher than the control groups. As shown in Fig. 6, there was a significant IgA response to CS-*MxiH* and Adj-*MxiH* compared to control groups, whereas, titer of IgA in *MxiH*-immunized group were not significantly different from the control groups (CS and PBS). The results indicated that after three-time vaccination with 20-day intervals, the levels of IgG and IgA effectively increased in the CS-*MxiH* and Adj-*MxiH* immunized groups (Fig. 7).

3.6. IL-4 and IFN-γ cytokines measurement

Quantitative ELISA method was used to measure the level of IFN-γ and IL-4 cytokines in antigen-activated splenocytes isolated from the immunized mice compared with negative controls. The results showed the highest level of IFN-γ in the group stimulated with CS-*MxiH*. In contrast, the level of IFN-γ production was not significantly different between two groups receiving Adj-*MxiH* and *MxiH*. Analyzing the production of IL-4 cytokines showed that the highest level was in the Adj-*MxiH* stimulated group. Furthermore, a considerable difference was found to produce the IL-4 cytokines in the groups receiving CS-*MxiH* and *MxiH*. As expected, the levels of IFN-γ and IL-4 cytokines in the control groups (CS and PBS) were lower than those in the antigen-stimulated groups.

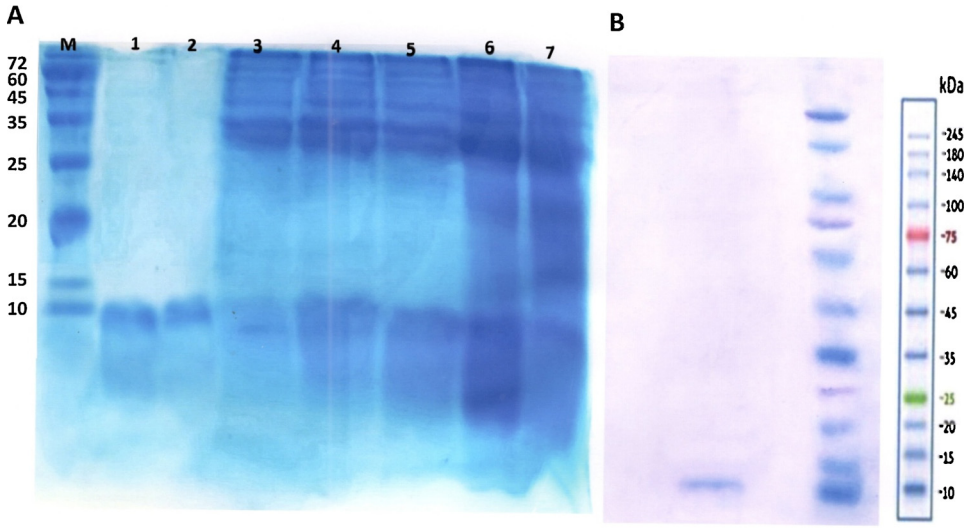

Fig. 2. Purification and Western blot analysis of recombinant protein (A) Purification steps of *MxiH* using NTA beads. M: proteinweight marker; Lane 1,2: purified *MxiH*-6X-His-tagged protein after elution with 250 mM imidazole. Lane 3, 4, 5: refolding step using urea (8 M) and arginine monohydrochloride and Lane 6, 7: total protein cell lysate after treating by lysis buffer. (B) Western blot carried out with anti-His-tagged antibodies, Lane1: His-tagged-*MxiH* protein; M: protein marker.

3.7. Challenge of immunized mice against

The intranasal administration of *MxiH* vaccine formulations showed a median survival of 6 for CS-*MxiH*, while *MxiH* and Adj-*MxiH* had 3 and 5 mice, respectively. In comparison with the negative control 10 % survival rate was observed and CS-*MxiH*, Adj-*MxiH* and *MxiH* yielded 60, 50 and 30 %, respectively (Fig. 8).

4. Discussion

Shigellosis is a common disease in developing countries, and with increasing antibiotic resistance, the need to prevent *Shigella* infection is felt more than ever. Despite extensive researches over the past decades, no effective vaccine founded against shigellosis (Akbari et al., 2019). Studies showed that the immune response to *Shigella* infection often triggered against O-antigen which is naturally limited to specific serotypes. However, the various *Shigella* antigens can be candidates for designing the vaccine, which wide spectrum immunity can be acquired against the common serotypes.

One of the most important antigens of the *Shigella* is *MxiH* that Deane et al. (2006) crystallized it to determine its three-dimensional structure. Studies have shown that vaccines derived from bacterial components and live attenuated *Shigella* cause weak and short-term immunity (Kotloff et al., 2018; Mirhoseini et al., 2018). Therefore, the incorporation of *Shigella* antigens with nanoparticles may enhance the immunogenicity potential of the various antigens (Zaharoff et al., 2007). In this study, pure *MxiH* antigen was used as nanoparticles based on low molecular weight CS.

Another important factor in designing the nanovaccine based on CS nanoparticles is its particle size. Several studies demonstrated that nanoparticles with positive charge and less than 500 nm in size represented suitable structure for vaccination (Gutierro et al., 2002; Najminejad et al., 2019). Studies showed that nanoparticle size could play a critical role in its penetration into the respiratory mucosa. As the particle size decreases, the effective dose of antigen reduced significantly. In this regard, Tsai et al. (2008) showed particles larger than

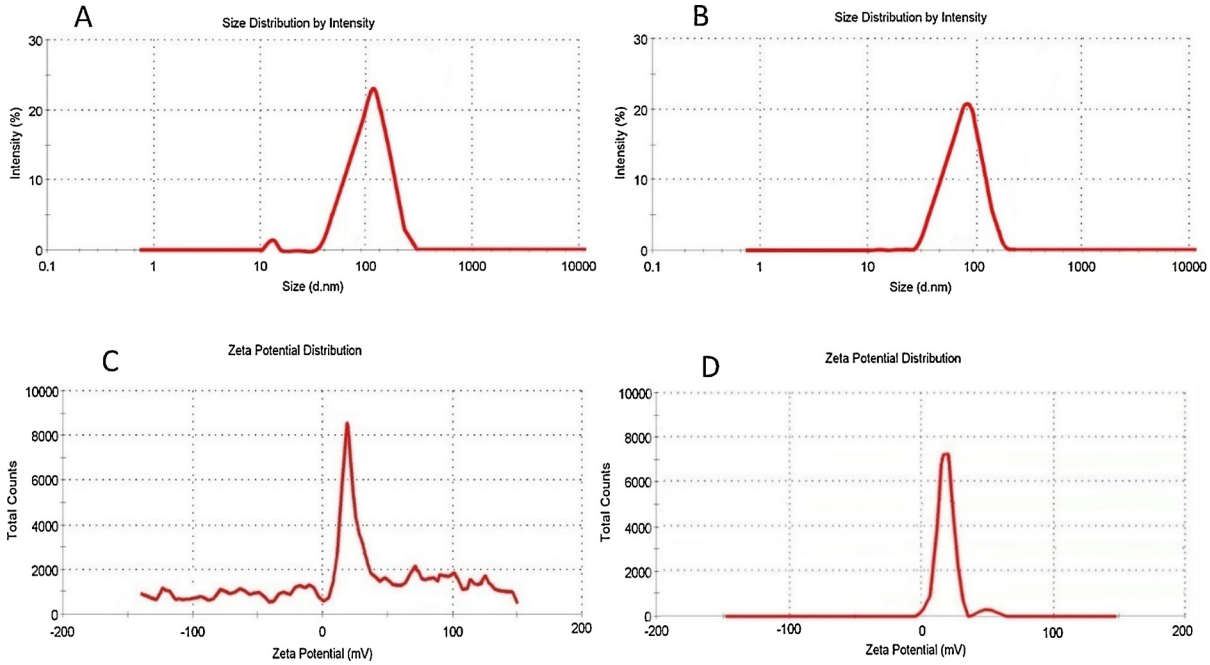

Fig. 3. Particle size distribution and surface charge of unloaded and *MxiH*-loaded CS. Size distribution measured of (A) CS and (B) CS-*MxiH*. Zeta potential of (C) CS and (D) CS-*MxiH*.

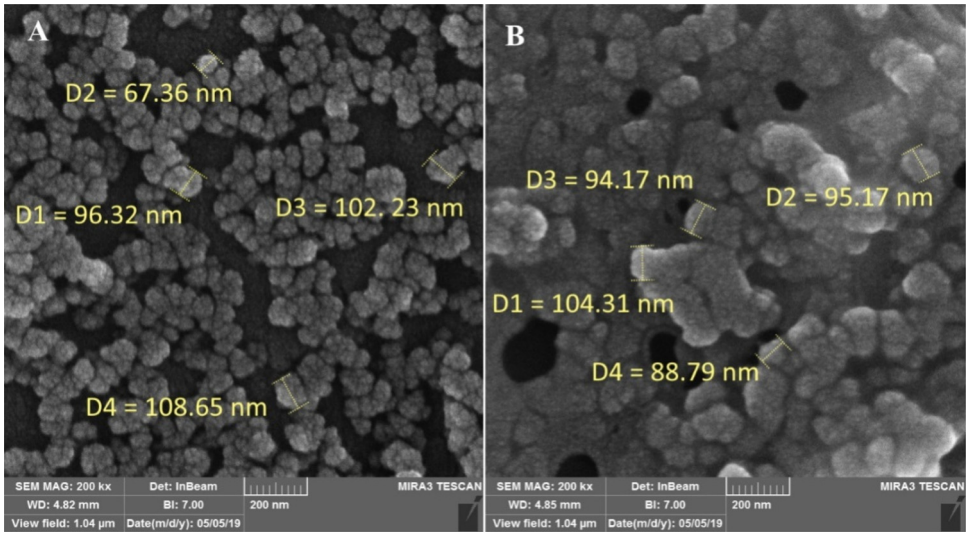

Fig. 4. SEM images of CS and Cs-*MxiH* nanoparticles. (A): unloaded CS and (B): *MxiH* loaded CS were about 100 nm in the nanosize.

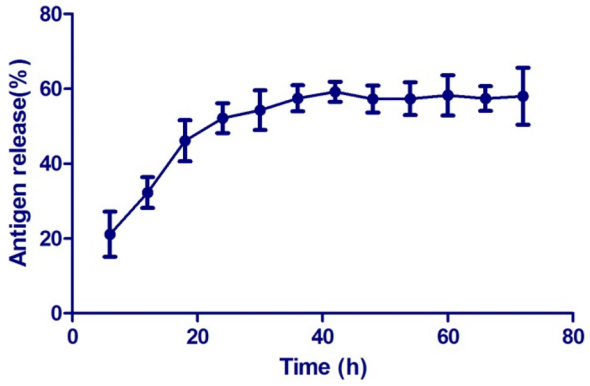

Fig. 5. In vitro release profile of *MxiH* antigen from Cs-*MxiH* at pH 7.4 at 37 °C for 72 h, calculated as a percentage release.

1 µm could not pass through the mucosal layer of the respiratory system, thus their exposure to the immune system get limited (Tsai et al., 2008). Another study showed that CS nanoparticles with a particle size of about 300 nm are easily captured by dendritic cells (DCs) (Paulis et al., 2013).

According to the results, the most desirable size distribution of nanoparticles was obtained in 0.3 % density of CS of. Compared to CS (control), the density of CS-*MxiH* decreased and its polydispersity did not change significantly by incorporating *MxiH* to CS. In this study, the negative net charge *MxiH* antigen reduced the size of the nanoparticles without altering its zeta potential when loaded in CS.

Intranasal vaccination of CS nanoparticles containing *MxiH* antigen increase M cells adsorption and nasal epithelial cells. Phagocytic cells in the nasal mucosa-associated lymphoid tissue facilitate antigen uptake and enhance the immune response (Doavi et al., 2016; Illum et al., 2001). The loading capacity of nanoparticles considered as a critical factor affecting the antigen immunogenicity.

As studies showed, the CS:Ag ratio may change the size of the nanoparticles and the amount of surface charge or one of them (Akbari et al., 2019). Gutierro et al. (2002) showed that when antigens are loaded on CS, the particle size increases. They also showed that the change in the zeta potential of the nanoparticles depends on the size of the antigen since no significant change in the zeta potential was observed with loading of BSA on the CS nanoparticles. In contrast, Hosseinzadeh et al. (2012) showed that both the size and potential of zeta decreased after protein loading in CS nanoparticles (Hosseinzadeh et al., 2012).

Based on DLS and zeta potential results, CS-*MxiH* nanoparticles had a positive charge and their size was estimated 50 − 200 nm. The zeta potential values obtained for CS nanoparticles after antigen loading were above 35 mV, which resulted in stable nanoparticles. Thus, the zeta potential and size of the nanoparticles obtained in this study are consistent with the findings of other studies (Amidi et al., 2006; Vila et al., 2004).

The in vitro release kinetic of *MxiH* antigen from CS nanoparticles showed that approximately 50 % of the antigen was released within 30 h. Prolonged-release of antigen in the nasal cavity results in increased uptake by mucosal and M cells, more efficient delivery to the mucosal lymph nodes, and then more efficient stimulation of APCs (Gregory et al., 2013). Since CS was found to increase the permeability of intercellular tight junctions, it seems that the stability of CS nanoparticles increases the uptake of loaded antigen by the nasal mucosa barrier (des Rieux et al., 2006; Vllasaliu et al., 2010). On the other hand, when CS nanoparticles penetrate the nasal mucosa, it is degraded by lysozyme and the residual encapsulated antigen is released (van der Lubben et al., 2001).

MxiH antigen showed high potential in activating the humoral immune cell-mediated immune system. CS-based nanovaccine formulation was found to significantly increase serum specific IgG and proliferation of CD^{4+} cells (Mehrabi et al., 2018; Wang et al., 2019). In this study, serum IgG and IgA titers in the experimental groups revealed that IgG titers were approximately twice that of IgA. On the other hand, IgA titers for CS-*MxiH* immunization were lower than in the Adj-*MxiH* group. Interestingly, IgG titer increased significantly in the third vaccination compared to the second while there was no significant difference in IgA production between the second and third vaccinations.

The immune cells in the nasal epithelium are myeloid and plasmacytoid types, which play a major role in phagocytosis and antigen presentation (Wang et al., 2019). These cells activate B-lymphocytes by secreting IL-6 and 12. Furthermore, plasmacytoid DC has the ability to secrete type-1 IFNs, which triggers natural killer cells to produce IFN-γ activating the differentiation of B cells (Martinez-Becerra et al., 2012; Siegal et al., 1999). Kotloff et al. (2000) reported that individuals who immunized with *S. flexneri* 2a strain CVD1207 induced an IFN-γ response (Kotloff et al., 2000). Samandari et al. (2000) showed that the immunity of individuals who were stimulated with *Shigella* bacterial antigens such as Ipa protein lead to the production of IFN-γ (Samandari et al., 2000).

Cytokine assay results indicated that those groups immunized with CS-*MxiH* and Adj-*MxiH* formulation had a high potential to produce IFN-γ and IL-4. Numerous studies have confirmed the effective role of

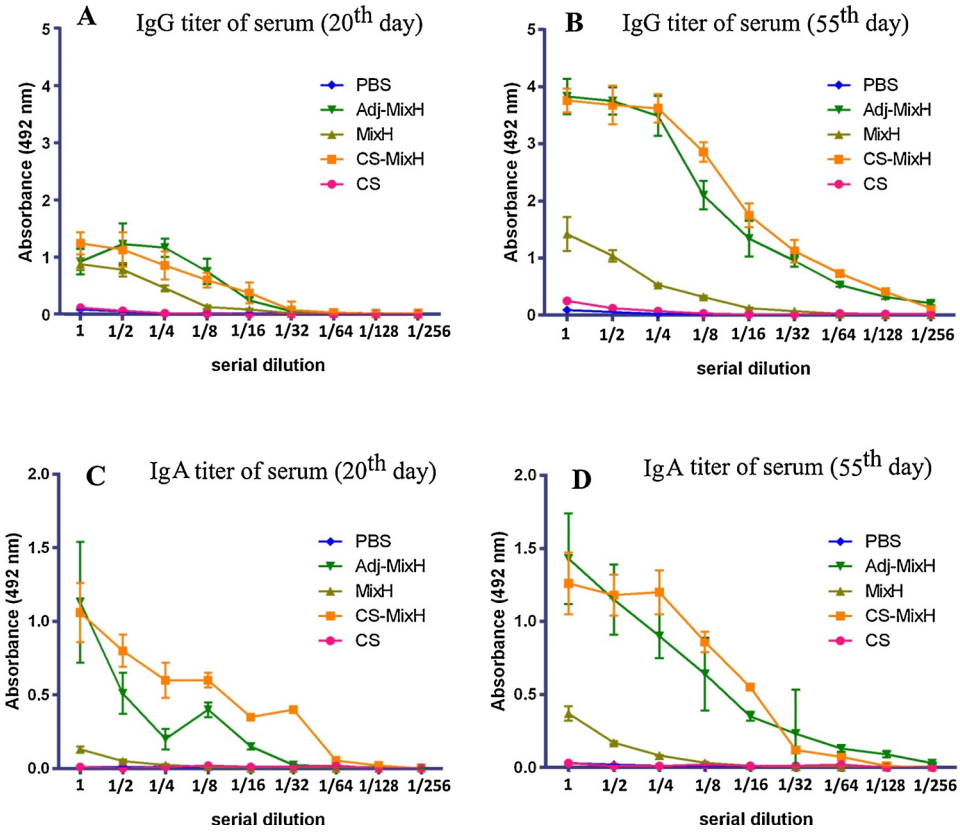

Fig. 6. Serum antibody levels in the groups of mice studied. (A) Serum IgG after the second vaccination on day 20 (b) IgG titers after the third vaccination on day 55. (C) Serum IgA after the second vaccination on day 20; (B) IgA titers after the third vaccination on day 55 measured in mice vaccinated by three formulations containing *MxiH* antigen and 2 controls.

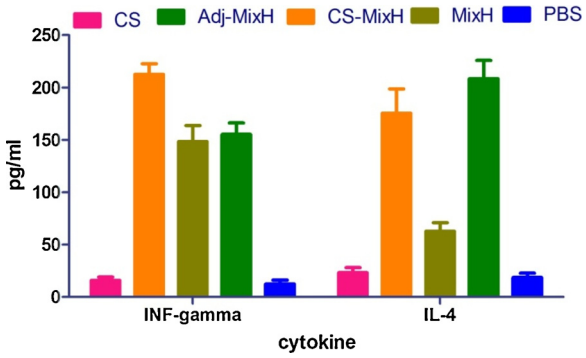

Fig. 7. The levels of IFN-γ and IL-4release from splenocytes of vaccinated mice. Titer values represent the mean ± SD of four mice per group.

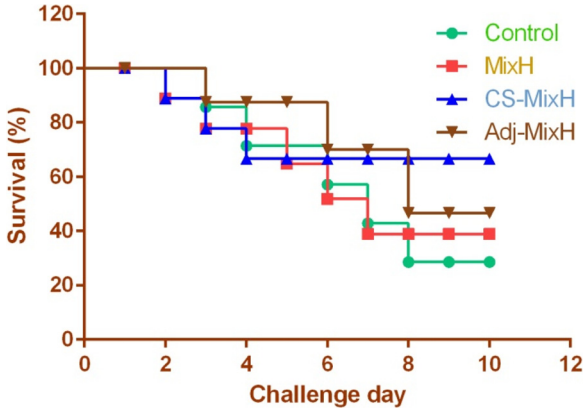

Fig. 8. Immunization against *Shigella* infection. Mice were challenged on day 60 after the first intranasal vaccination. Results are obtained from survival percentage for 10 mice in each group.

these two cytokines to activate the humoral immune system (Ashkenazi & Cohen, 2013; Granato et al., 2014; Wang et al., 2019).

According to the results, the intranasal administration of *MxiH* antigen resulted in high serum levels of INF-γ and IL-4, which may stimulate humoral immunity and induce differentiation of B cells into plasmocytes. These findings are consistent with some studies that used CS-based nanovaccines for immunization in mice as an animal model (Doavi et al., 2016; Fasihi-Ramandi et al., 2018; Khanifar et al., 2019).

The results of the challenge assay were consistent with the data obtained from the humoral immunity assay so that groups with high survival rates were immunized with CS-*MxiH* and Adj-*MxiH*.In addition, the levels of humoral immunity and cytokines stimulating antibody production were significantly higher in the groups immunized with CS-*MxiH* and Adj-*MxiH*.

5. Conclusion

These findings suggested that the loading of *MxiH* antigen in CS nanoparticles could provide some benefits as an efficient vaccine to enhance immunity to *Shigella* infection. Likewise, given the increased levels of IgG and IgA in mice exposed to intranasal administration of CS-*MxiH*, it can be concluded that vaccines-based CS nanoparticles have a strong immunogenic ability to stimulate humoral and mucosal immunity.

Authors' contributions

Farhad Gliavand performed the study as major researcher. Abdolrazagh Marzban was responsible for data arrangements, scientific writing and graphical designing. Neda Soleimani contributed to proposal design and experiments. animal studies, Golamhossein Ebrahimipour was the first supervisor in the thesis and Mehdi Goudarzi supported the thesis financially as a second supervisor.

Acknowledgments

This research was performed as part of master thesis of Mr. Farhad Gilavand and was financially supported by the grant (No 9393) from Research Deputy of Shahid Beheshti University of Medical Sciences, Tehran, Iran. The authors thank Razi Herbal Medicine Research Center, Lorestan University of Medical Sciences for their assistance in completing the studies.

References

Akbari, M. R., Saadati, M., Honari, H., & Ghorbani, H. M. (2019). IpaD-loaded N-trimethyl chitosan nanoparticles can efficiently protect guinea pigs against Shigella flexneri. *Iranian Journal of Immunology: IJI, 16*(3), 212–224.

Ashrafi, B., Rashidipour, M., Marzban, A., Soroush, S., Azadpour, M., Delfani, S., & Ramak, P. (2019). Mentha piperita essential oils loaded in a chitosan nanogel with inhibitory effect on biofilm formation against S. Mutans on the dental surface. *Carbohydrate Polymers, 212*, 142–149.

Amidi, M., Romeijn, S. G., Borchard, G., Junginger, H. E., Hennink, W. E., & Jiskoot, W. (2006). Preparation and characterization of protein-loaded N-trimethyl chitosan nanoparticles as nasal delivery system. *Journal of Controlled Release, 111*(1-2), 107–116.

Amini, Y., Tebianian, M., Mosavari, N., Fasihi Ramandi, M., Ebrahimi, S. M., Najminejad, H., & Abdollahpour, M. (2017). Development of an effective delivery system for intranasal immunization against Mycobacterium tuberculosis ESAT-6 antigen. *Artificial Cells, Nanomedicine, and Biotechnology, 45*(2), 291–296.

Ashkenazi, S., & Cohen, D. (2013). An update on vaccines against *Shigella*. *Therapeutic Advances in Vaccines, 1*(3), 113–123.

Barry, E. M., Pasetti, M. F., Sztein, M. B., Fasano, A., Kotloff, K. L., & Levine, M. M. (2013). Progress and pitfalls in Shigella vaccine research. *Nature Reviews Gastroenterology & Hepatology, 10*(4), 245.

Bohn, E., Sonnabend, M., Klein, K., & Autenrieth, I. B. (2019). Bacterial adhesion and host cell factors leading to effector protein injection by type III secretion system. *International Journal of Medical Microbiology, 309*(5), 344–350.

Bradford, M. M. (1976). A rapid and sensitive method for the quantitation of microgram quantities of protein utilizing the principle of protein-dye binding. *Analytical Biochemistry, 72*(1-2), 248–254.

Camacho, A. I., Irache, J. M., & Gamazo, C. (2013). Recent progress towards development of a *Shigella* vaccine. *Expert Review of Vaccines, 12*(1), 43–55.

Deane, J. E., Roversi, P., Cordes, F. S., Johnson, S., Kenjale, R., Daniell, S., et al. (2006). Molecular model of a type III secretion system needle: Implications for host-cell sensing. *Proceedings of the National Academy of Sciences, 103*(33), 12529–12533.

Des Rieux, A., Fievez, V., Garinot, M., Schneider, Y.-J., & Préat, V. (2006). Nanoparticles as potential oral delivery systems of proteins and vaccines: A mechanistic approach. *Journal of Controlled Release, 116*(1), 1–27.

Doavi, T., Mousavi, S. L., Kamali, M., Amani, J., & Ramandi, M. F. (2016). Chitosan-based intranasal vaccine against Escherichia coli O157: H7. *Iranian Biomedical Journal, 20*(2), 97.

Fasihi-Ramandi, M., Ghobadi-Ghadikolaee, H., Ahmadi-Renani, S., Taheri, R. A., & Ahmadi, K. (2018). Vibrio cholerae lipopolysaccharide loaded chitosan nanoparticle could save life by induction of specific immunoglobulin isotype. *Artificial Cells, Nanomedicine, and Biotechnology, 46*(1), 56–61.

Granato, A., Hayashi, E. A., Baptista, B. J., Bellio, M., & Nobrega, A. (2014). IL-4 regulates Bim expression and promotes B cell maturation in synergy with BAFF conferring resistance to cell death at negative selection checkpoints. *The Journal of Immunology, 192*(12), 5761–5775.

Gregory, A. E., Williamson, D., & Titball, R. (2013). Vaccine delivery using nanoparticles. *Frontiers in Cellular and Infection Microbiology, 3*, 13.

Gutierro, I., Hernandez, R., Igartua, M., Gascon, A., & Pedraz, J. (2002). Size dependent immune response after subcutaneous, oral and intranasal administration of BSA loaded nanospheres. *Vaccine, 21*(1-2), 67–77.

Hosseinzadeh, H., Atyabi, F., Dinarvand, R., & Ostad, S. N. (2012). Chitosan–Pluronic nanoparticles as oral delivery of anticancer gemcitabine: Preparation and in vitro study. *International Journal of Nanomedicine, 7*, 1851.

Illum, L., Jabbal-Gill, I., Hinchcliffe, M., Fisher, A., & Davis, S. (2001). Chitosan as a novel nasal delivery system for vaccines. *Advanced Drug Delivery Reviews, 51*(1-3), 81–96.

Jahantigh, D., Saadati, M., Fasihi-Ramandi, M., Mousavi, M., & Zand, A. M. (2014). Novel intranasal vaccine delivery system by chitosan nanofibrous membrane containing N-terminal region of IpaD antigen as a nasal Shigellosis vaccine, Studies in Guinea pigs. *Journal of Drug Delivery Science and Technology, 24*(1), 33–39.

Kaminski, R. W., & Oaks, E. V. (2009). Inactivated and subunit vaccines to prevent shigellosis. *Expert Review of Vaccines, 8*(12), 1693–1704.

Kang, M. L., Jiang, H. L., Kang, S. G., Guo, D. D., Lee, D. Y., Cho, C. S., et al. (2007). Pluronic F127 enhances the effect as an adjuvant of chitosan microspheres in theintranasal delivery of*Bordetella bronchisepticaantigens containing dermonecrotoxin. *Vaccine, 25*(23), 4602–4610.

Kazemi, R., Akhavian, A., Amani, J., Salimian, J., Motamedi, M.-J., Mousavi, A., et al. (2016). Immunogenic properties of trivalent recombinant protein composed of B-subunits of LT, STX-2, and CT toxins. *Microbes and Infection, 18*(6), 421–429.

Khanifar, J., Salmanian, A. H., Haji Hosseini, R., Amani, J., & Kazemi, R. (2019). Chitosan nano-structure loaded with recombinant E. Coli O157: H7 antigens as a vaccine candidate can effectively increase immunization capacity. *Artificial Cells, Nanomedicine, and Biotechnology, 47*(1), 2593–2604.

Kotloff, K. L., Noriega, F. R., Samandari, T., Sztein, M. B., Losonsky, G. A., Nataro, J. P., et al. (2000). Shigella flexneri 2a Strain CVD 1207, with Specific Deletions in virG, sen, set, andguaBA, is highly attenuated in Humans. *Infection and Immunity, 68*(3), 1034–1039.

Kotloff, K. L., Riddle, M., Platts-Mills, J. A., Pavlinac, P., & Zaidi, A. K. M. (2018). Shigellosis. *Lancet, 391*(10122), 801–812.

Levine, M. M., Kotloff, K. L., Barry, E. M., Pasetti, M. F., & Sztein, M. B. (2007). Clinical trials of Shigella vaccines: Two steps forward and one step back on a long, hard road. *Nature Reviews Microbiology, 5*(7), 540.

Marandi, B. H. G., Zolfaghari, M. R., Kazemi, R., Motamedi, M. J., & Amani, J. (2019). Immunization against Vibrio cholerae, ETEC, and EHEC with chitosan nanoparticle containing LSC chimeric protein. *Microbial Pathogenesis*103600.

Martinez-Becerra, F. J., Kissmann, J. M., Diaz-McNair, J., Choudhari, S. P., Quick, A. M., Mellado-Sanchez, G., et al. (2012). Broadly protective Shigella vaccine based on type III secretion apparatus proteins. *Infection and Immunity, 80*(3), 1222–1231.

Mehrabi, M., Montazeri, H., Mohamadpour Dounighi, N., Rashti, A., & Vakili-Ghartavol, R. (2018). Chitosan-based nanoparticles in mucosal vaccine delivery. *Archives of Razi Institute, 73*(3), 165–176.

Mirhoseini, A., Amani, J., & Nazarian, S. (2018). Review on pathogenicity mechanism of enterotoxigenic Escherichia coli and vaccines against it. *Microbial Pathogenesis, 117*, 162–169.

Najminejad, H., Kalantar, S. M., Mokarram, A. R., Dabaghian, M., Abdollahpour-Alitappeh, M., Ebrahimi, S. M., et al. (2019). *Bordetella pertussis* antigens encapsulated into N-trimethyl chitosan nanoparticulate systems as a novel intranasal pertussis vaccine. *Artificial Cells, Nanomedicine, and Biotechnology, 47*(1), 2605–2611.

Paulis, L. E., Mandal, S., Kreutz, M., & Figdor, C. G. (2013). Dendritic cell-based nanovaccines for cancer immunotherapy. *Current Opinion in Immunology, 25*(3), 389–395.

Samandari, T., Kotloff, K. L., Losonsky, G. A., Picking, W. D., Sansonetti, P. J., Levine, M. M., & Sztein, M. B. (2000). Production of IFN-γ and IL-10 to Shigella invasins by mononuclear cells from volunteers orally inoculated with a shiga toxin-deleted Shigella dysenteriae type 1 strain. *The Journal of Immunology, 164*(4), 2221–2232.

Siegal, F. P., Kadowaki, N., Shodell, M., Fitzgerald-Bocarsly, P. A., Shah, K., Ho, S., et al. (1999). The nature of the principal type 1 interferon-producing cells in human blood. *Science, 284*(5421), 1835–1837.

Taranejoo, S., Janmaleki, M., Rafienia, M., Kamali, M., & Mansouri, M. (2011). Chitosan microparticles loaded with exotoxin A subunit antigen for intranasal vaccination against Pseudomonas aeruginosa: An in vitro study. *Carbohydrate Polymers, 83*(4), 1854–1861 1.

Tsai, M. L., Bai, S. W., & Chen, R. H. (2008). Cavitation effects versus stretch effects resulted in different size and polydispersity of ionotropic gelation chitosan–sodium tripolyphosphate nanoparticle. *Carbohydrate Polymers, 71*(3), 448–457.

Van der Lubben, I. M., Verhoef, J. C., Borchard, G., & Junginger, H. E. (2001). Chitosan and its derivatives in mucosal drug and vaccine delivery. *European Journal of Pharmaceutical Sciences, 14*(3), 201–207.

Vila, A., Sánchez, A., Janes, K., Behrens, I., Kissel, T., Jato, J. L. V., & Alonso, M. J. (2004). Low molecular weight chitosan nanoparticles as new carriers for nasal vaccine delivery in mice. *European Journal of Pharmaceutics and Biopharmaceutics, 57*(1), 123–131.

Vllasaliu, D., Exposito-Harris, R., Heras, A., Casettari, L., Garnett, M., Illum, L., & Stolnik, S. (2010). Tight junction modulation by chitosan nanoparticles: Comparison with chitosan solution. *International Journal of Pharmaceutics, 400*(1-2), 183–193.

Wang, H., Breed, E. R., Lee, Y. J., Qian, L. J., Jameson, S. C., & Hogquist, K. A. (2019). Myeloid cells activate iNKT cells to produce IL-4 in the thymic medulla. *Proceedings of the National Academy of Sciences*201910412.

Zaharoff, D. A., Rogers, C. J., Hance, K. W., Schlom, J., & Greiner, J. W. (2007). Chitosan solution enhances both humoral and cell-mediated immune responses to subcutaneous vaccination. *Vaccine, 25*(11), 2085–2094.